HHS Public Access

Author manuscript

Sci Transl Med. Author manuscript; available in PMC 2015 August 07.

Published in final edited form as:

Sci Transl Med. 2010 July 28; 2(42): 42ra53. doi:10.1126/scitranslmed.3001148.

Function of an Implanted Tissue Glucose Sensor for More than One Year in Animals

David A. Gough[ϕ,*], **Lucas S. Kumosa**[ϕ], **Timothy L. Routh**[ζ], **Joe T. Lin**[ζ], and **Joseph Y. Lucisano**[ζ]

[ϕ]Department of Bioengineering, University of California San Diego, 9500 Gilman Drive, La Jolla, CA 92093-0412

[ζ]GlySens Incorporated, 6450 Lusk Blvd., Suite E-109, San Diego, CA 92121

Abstract

An implantable sensor capable of long-term monitoring of tissue glucose concentrations by wireless telemetry has been developed for eventual application in people with diabetes. In a recent trial, the sensor-telemetry system functioned continuously while implanted in subcutaneous tissues of two pigs for a total of 222 days and 520 days respectively, with each animal in both non-diabetic and diabetic states. The sensor detects glucose via an enzyme electrode principle that is based on differential electrochemical oxygen detection, which reduces the sensitivity of the sensor to encapsulation by the body, variations in local microvascular perfusion, limited availability of tissue oxygen, and inactivation of the enzymes. After an initial two-week stabilization period, the implanted sensors maintained stability of calibration for extended periods. The lag between blood and tissue glucose concentrations was 11.8 ± 5.7 minutes and 6.5 ± 13.3 minutes respectively, for rising and falling blood glucose challenges (mean ± SD). The lag was determined mainly by glucose mass transfer in the tissues, rather than the intrinsic response of the sensor, and showed no systematic change over implant test periods. These results represent a milestone in the translation of the sensor system to human applications.

INTRODUCTION

Diabetes is a major health problem that results in significant mortality, debilitating complications, substantial economic impact on society, and untold waste of human resources (1). The results of the prospective Diabetes Control and Complications Trial show that complications of diabetes can be significantly reduced by improved blood glucose control (2). However, this conclusion is problematic for most people with the disease because the

[*]Address correspondence to: Dr. David Gough, Department of Bioengineering, University of California San Diego, 9500 Gilman Drive, La Jolla, CA 92093-0412 Phone: (858)-822-3446. Fax: (858)-534-5722. dgough@ucsd.edu.

An implanted tissue glucose sensor can provide stable readings of glucose concentrations on a long-term basis.

Author contributions: sensor design was done by D.A.G., J.Y.L., J.T.L., and T.L.R.; animal studies were conducted by J.T.L., T.L.R., and J.Y.L.; histology samples were processed and images prepared by L.S.K.; device fabrication was carried out by T.L.R., J.T.L., and J.Y.L.; all authors participated in data analysis and manuscript preparation.

Competing interests: D.A.G. is founder and consultant to GlySens, an arrangement approved by the University of California San Diego in accordance with its conflict of interest policies. The authors have equity interests in GlySens. GlySens is the owner and developer of the device and licensee of intellectual property for some aspects of the technology from UCSD.

most common means for measurement of blood glucose involves blood collection by "fingersticking," a method that is inconvenient and unacceptable to many people with diabetes, and is rarely performed frequently enough to follow blood glucose dynamics.

Continuous glucose monitoring with short-term, percutaneous glucose sensors is a currently available alternative (3), although it has certain drawbacks. These sensors are inserted in subcutaneous tissues using needle introducers and remain in place for 3 to 7 days before being replaced. Their performance can be affected by changes known to occur in the tissues due to the insertion and presence of the implant (4), which can result in instability of the glucose signal, and fingerstick glucose assays are needed for regular sensor recalibration during use. These sensors have therefore not been approved by the FDA as a primary standard for glucose measurement and cannot be fully relied upon to warn the user of an impending hypoglycemic episode (5). Nevertheless, an important result of the use of short-term subcutaneous glucose sensors is the realization that blood glucose varies to a much greater extent during the course of the day than was previously thought, even in presumed well-controlled individuals. These sensors have also made possible initial clinical research on the artificial pancreas (for example, 6).

For acceptance by a broader group of users, there is a need for a long-term, totally implanted glucose sensor and wireless telemetry system. The implant should monitor tissue glucose continuously and report via telemetry to an external receiver that could display the blood glucose information or relay it to a caregiver. This information could be used in a number of ways to help achieve improved blood glucose control: it could direct dosing of therapeutics, warn of hypoglycemia, guide diet modification and exercise, or act as an input to an artificial pancreas. It could also be used in conjunction with other forms of therapy such as drugs, transplants, islet replacement or preservation, or stem cells. To be optimally acceptable by users, the sensor should function for a year or more, be insertable by a simple outpatient procedure requiring only local anesthesia, be convenient and unobtrusive, be free of significant risk for untoward effects, and not require frequent recalibration.

We report here long-term tissue glucose monitoring with a sensor-telemetry system implanted in subcutaneous tissues of pigs. Monitoring was carried out while pigs were non-diabetic (for three weeks in one animal and nearly one year in the other) and, after the pigs had been converted to insulin-dependent diabetic by administration of streptozotocin (STZ), monitoring continued in each animal for an additional six months, with diabetes managed by insulin injection and diet control.

RESULTS

Sensing Principle

The glucose sensor is based on the following two-step chemical reaction catalyzed by glucose oxidase and catalase (7):

$$\text{glucose} + O_2 + H_2O \rightarrow \text{gluconic acid} + H_2O_2$$

$$H_2O_2 \rightarrow \tfrac{1}{2}\, O_2 + H_2O$$

resulting in the overall enzyme reaction:

$$\text{glucose} + \tfrac{1}{2}\, O_2 \rightarrow \text{gluconic acid}$$

The two enzymes are immobilized within a crosslinked protein gel that is in contact with an electrochemical oxygen sensor. Glucose and ambient oxygen diffuse into the gel, encounter the enzymes, the above reactions occur, and oxygen that is not consumed in the process is detected by the sensor. After comparison with the background oxygen concentration detected by a separate oxygen reference sensor, the difference is related to glucose concentration. The sensing unit is therefore composed of: (i) a glucose sensor, which is an oxygen sensor with an immobilized enzyme gel that produces a glucose-modulated, oxygen-dependent current, *igmo*; (ii) a reference oxygen sensor without enzymes that produces an oxygen-dependent current, *io*; and (iii) a signal processing element that takes the difference of (i) and (ii) to give the signal of interest, the glucose-dependent difference current, *ig*.

The sensor is calibrated with the formula $BG=k_1 i_o F(k_2 \bullet i_g/i_o)$, where BG is blood glucose, k_1 is the oxygen mass transfer coefficient for the reference sensor, k_2 is the glucose mass transfer coefficient related to the implant environment, and F is a quasi-linear sensitivity function of the glucose sensor determined *in vitro*. With an appropriately designed immobilized enzyme gel structure (8), the sensor can remain responsive to glucose in the tissue implant environment over clinically relevant concentration ranges. This calibration relationship is an adaptation of our previous methods (9, 10).

The Implant

Eight 300-μm platinum working electrodes, with associated platinum counter electrodes and Ag/AgCl potential reference electrodes, are arranged as four sensor pairs on the surface of a 1.2-cm diameter alumina disc (11). The electrodes are covered by a thin electrolyte layer, a protective layer of medical grade polydimethylsiloxane (PDMS), and a membrane of PDMS with wells for the immobilized enzymes located over certain electrodes. The enzymes are immobilized in the wells by crosslinking with albumin using glutaraldehyde, and the resulting gel is rinsed extensively to remove unbound material. The alumina disc is fused into a hermetically sealed titanium housing (Fig. 1) containing a potentiostat and signal conditioning circuitry for each sensor, a wireless telemetry system, and a battery having a minimum 1-year lifetime. The implant is sterilized with a chemical sterilant using a procedure that has been validated according to standard methods (12).

The telemetry system samples the currents from individual sensors, encodes the samples into multiplexed signal segments, and transmits the segments as a train of radio frequency signals at regular 2-minute intervals to an external receiver, where the signals are decoded and recorded. The potentiostat circuitry in the implant is based on an electronic design described in detail elsewhere (13), extended in this case for control of 8 individual working electrodes. Radio telemetry is accomplished using a 433.92 MHz carrier signal with a total effective radiated power of less than 100 nanowatts, providing a practical effective transmitter range of approximately 10 feet with information packet reception rate exceeding 97%. This hermetically sealed wireless telemetry system makes possible long-term recordings without infection-prone percutaneous electrical leads.

Implantation

Two series of implant studies were conducted. In the first series, intended to aid design optimization and component reliability verification, a total of 30 individual sensor-telemetry units were implanted in six non-diabetic pigs to refine the surgical technique, evaluate device tolerance and biocompatibility, test the electronic circuitry and telemetry, and identify factors that affect the lifetime of the sensor. The devices in this series were explanted and analyzed according to pre-set protocol schedules at periods ranging from one to eighteen months after implantation. Results from this foundational research included verification of: (a) acceptable long-term biocompatibility, assessed following 18-month implant periods; (b) immobilized enzyme life exceeding one year; (c) battery life exceeding one year; (d) electronic circuitry reliability and telemetry performance; (e) sensor mechanical robustness including long-term maintenance of hermeticity; (f) stability of the electrochemical detector structure; and (g) acceptability and tolerance of the animals to the implanted device. Results were also obtained from this series related to the effects of tissue permeability and tissue remodeling, and are reported below.

In the second series, which involved evaluation under diabetic conditions and which is described in detail here, two devices were implanted in each of two pigs (4 devices total), and first operated for 352 days (Subject #1) and 16 days (Subject #2) respectively, with the animals in the non-diabetic state. The animals were then made diabetic by administration of STZ, and the devices continued to operate for an additional 168 days in Subject #1 to a total of 520 days, and for an additional 206 days in Subject #2 to a total of 222 days. Individual experiments were terminated based on consideration of the resources required to maintain diabetic animals.

No adverse medical events (infection, erosion, migration, etc.) were encountered with any implant in either test series. Together, the test series represent a collective 31 total device-years of implant experience, with 17 of the devices remaining implanted and functional for more than one year.

Glucose Sensor Recordings

The sensor response in Subject #1 over a five week period during the non-diabetic phase is shown in Fig. 2. In this example, only one system calibration adjustment was performed during the period (on day 186), with the goal of obtaining a qualitative indication of the implanted sensor stability. From that point forward, a fixed calibration regimen with regular calibration adjustment every 10 days was employed for analysis of sensor accuracy (see below). A practical recalibration schedule will need to be established later for human use.

Results after the pigs became diabetic are also shown in Fig. 2. As expected, we noted a considerable difference in the extent and duration of glucose excursions between the non-diabetic and diabetic states. In the non-diabetic state, glucose concentration remained relatively constant at a baseline of approximately 75 mg/dL, regardless of feeding and physical activity. As a result, to test the sensor sensitivity to glucose, it was necessary to create blood glucose excursions by intravenous infusion of glucose, resulting in rapid rise and rapid unaided return to the baseline caused by the endogenous insulin response. In the

diabetic state however, the blood glucose concentration varied substantially with time, rising and falling in complex response to feeding, activity, and administration of insulin. (Note that the sensor response was electronically “capped” at 400 mg/dL, so glucose values above that level are not reported by the sensor.) Insulin injections were needed regularly to interrupt sustained hyperglycemia episodes.

Accuracy

We assessed the sensor accuracy on the basis of data collected from glucose excursion tests conducted during the diabetic phase in Subjects #1 and #2. Conventional statistical methods were employed, including standard regression analysis (14), error grid plots that segregate results into graphical regions on the basis of potential clinical significance by using both original sensor values and values adjusted for delay (described below) (15), and mean and median absolute relative difference (ARD) analyses (16). Results obtained from the diabetic animals are as follows (with values retrospectively adjusted for an average 6.6-minute delay, determined for the diabetic phase as discussed below, in parentheses): number of points: 392; error grid values: 63.8% (70.4%) of points in region A, 32.4% (28.6%) in region B (clinically benign), 3.6% (1.0%) in region C, 0.3% (zero) in region D, and zero (zero) in region E (potentially dangerous clinically); ARD values: mean 22.1% (17.9%), median 14.7% (13.2%); and correlation coefficient: 0.88 (0.92). These results suggest that although there may be quantifiable differences between the actual blood glucose concentrations and values reported by the sensor, none of these differences would lead to a mistaken, potentially dangerous clinical action. The results obtained here are comparable to published values obtained for shorter periods from currently available short-term continuous glucose monitors used clinically (16, 17).

Signal Delay

When sensors are operated continuously, a lag or delay exists during dynamic conditions between the actual blood glucose concentration and the value reported by the sensor. Associated with the delay is the dynamic error, which is the difference between the actual and reported blood glucose values at a given time (18). The delay and associated error can depend on the intrinsic rate of the sensor response, the rate of glucose mass transfer in the tissues, and the instantaneous rate of blood glucose change of the subject (18). The component of delay due to the sensor is determined from *in vitro* experiments in which glucose concentration is changed abruptly. The instantaneous rate of blood glucose change is determined by frequent blood glucose sampling, and the rate of glucose mass transfer in the tissues is limiting when the other two processes are much faster.

The delay in the response to an IVGTT in Subject #1 on day 168 during the non-diabetic phase is shown in Fig. 3. The maximal rate of glucose rise due to glucose infusion was approximately 8 mg/dL•min^{-1} and the maximal rate of fall, due to endogenous insulin action, was 6 mg/dL•min^{-1}. After an initial lag, the sensor signal rose at a rate parallel to the plasma glucose ramp. The glucose concentration then remained at a plateau value of approximately 260 mg/dL created by a reduced glucose infusion rate for about 15 minutes, before falling toward the baseline, with the sensor signal falling thereafter. During the excursion tests in the diabetic phases, maximal rates of central venous plasma glucose

change (mean ± SD) were 4.1 ± 1.9 and 5.2 ± 1.0 mg/dL•min^{-1} for rising and falling transitions, respectively. The rates of blood glucose change during testing in the non-diabetic phases were significantly more rapid than the maximal spontaneous rates of change reported in diabetic subjects (19), which are approximately 3 mg/dL•min^{-1} rising, and 2.5 mg/dL•min^{-1} falling.

The definition of the rising or falling delay used here (shown by the arrows in Fig. 3) is the time between the plasma glucose value and the sensor value at the 50% point between the minimum and maximum plasma glucose values in an excursion. For example, if the minimum plasma glucose value in an excursion was 100 mg/dL (e.g. at baseline, prior to infusion of glucose) and reached a plateau at 200 mg/dL upon glucose infusion, the rising delay is the difference between the time the plasma glucose reaches 150 mg/dl and the time that the sensor indicates 150 mg/dl. The falling delay from each excursion was evaluated during the falling leg at the same 50% plasma glucose crossing point. Using this technique, the average value of the rising delay was 11.8 ± 5.7 minutes (mean ± SD) and of the falling delay was 6.5 ± 13.3 minutes, based on 34 IVGTTs in Subject #1 during the non-diabetic period. Of these values, 2.5 ± 1.2 minutes is ascribable to the sensor itself, as determined from independent *in vitro* measurements, and an estimated 0.5 minutes is ascribable to circulatory transport from the central venous infusion site to the implant site. The remainders of the rising and falling average delays (8.8 and 3.5 minutes, respectively) are attributable to mass transfer and physiologic phenomena within the local tissues. Over the extended implant period, there was no trend in either average delay value.

We confirmed these delay values with an alternative approach (20) based on systematic retrospective displacement of the sensor signal values with respect to the measured plasma glucose values and determination of the root mean square coefficient of variation between all sensor and plasma values at each step. For the 34 IVGTT data set of Subject #1 referenced above, the minimum coefficient of variation value was obtained at a signal displacement of approximately 10 minutes, which is comparable to the average of the rising and falling lag values determined as reported above. In the diabetic phase, the minimum coefficient of variation value was obtained at a signal displacement of 6.6 minutes (average of Subject #1 and #2).

Oxygen Reference Sensor

Signals from the oxygen reference sensor indicate the time-course of change in tissue permeability after implantation. The averaged signals from the oxygen reference sensors from the first series of implanted animals are plotted as a function of implant time in weeks (Fig. 4). Each data point (open circle) represents an average of 60 sensor signals at the indicated time after implantation, and points are fitted to an exponential decay curve (black line). It is noteworthy that the averaged oxygen signals decay exponentially, asymptotically approaching a non-zero value within about six weeks, and remain relatively constant thereafter. It has been shown previously in studies with hamsters (21) that the exponential signal decay is due to changes in the effective permeability of the tissue, rather than changes in the sensitivity of the sensors *per se*. This was demonstrated in (21) by comparison of pre-implantation and post-explantation measurements of sensor sensitivity to oxygen in the gas

phase, where boundary layers are absent and highly precise measurements are possible. Thus, the decay of both the oxygen reference signal and the oxygen component of the glucose sensor signal are due to changes in the effective permeability of the tissue, which stabilizes within several weeks.

The observation that the sensitivity to glucose remains stable during a period of significant oxygen signal decay reveals an important advantage of our sensor design. The glucose sensing strategy used here, which is based on differential oxygen detection, reduces the sensitivity of the glucose-dependent signal to tissue encapsulation by the foreign body response to the implant. Because the substrate sensitivity of both sensors decays in parallel as the effective tissue permeability decreases after implantation, the glucose-dependent difference signal remains largely unaffected.

Tissue Remodeling

Five millimeter-thick tissue samples were collected from two pigs in the first series at the time of implant removal on day 91, fixed using standard methods (see Materials and Methods), and stained with H&E and Gomori Trichrome stains and antibodies to visualize nuclear density, collagen density, and microvascular density (Fig. 5). Medical grade titanium, a well-known biocompatible material (22) that we used for the implant housing, served as a control. Nuclear density and collagen density are shown for tissues adjacent to the PDMS membrane surface (upper panels) and titanium surface (lower panels). The quantitative results (mean ± SD) were: nuclear (or cell) density 1282 ± 201 nuclei / mm^2 for tissue adjacent to the PDMS surface and 2769 ± 491 nuclei / mm^2 adjacent to the titanium control; collagen density 95.9 ± 2.1% (area ratio) adjacent to the PDMS surface and 53.1 ± 7.7% adjacent to the titanium control; microvascular density 0.05 ± 0.08% (area ratio) adjacent to the PDMS surface and 0.04 ± 0.06% adjacent to the titanium surface. The lower nuclear density and higher collagen density adjacent to the PDMS surface indicates a greater degree of tissue remodeling adjacent to the PDMS material compared to the titanium surface. However, microvascular density was comparable for the two materials, and microvessels necessary for mass transfer were present within a short distance from the implant surface.

DISCUSSION

Design for Long-term Function

This sensor has several important design features that make possible long-term operation in the tissue environment. First, glucose oxidase is specific for glucose over other biochemicals present in tissue fluids, and with proper design, the sensor can therefore also be specific. Second, there is a non-porous, PDMS layer between the enzyme membrane and the electrodes, which allows oxygen passage by solubilization in its hydrophobic phase, but prevents electrode poisoning and interference from polar endogenous biochemicals and common exogenous chemicals such as acetaminophen and ascorbic acid. Third, the electrochemical oxygen sensors are based on the three-electrode potentiostatic principle (23) and retain long-term stability of oxygen sensitivity, in contrast to some conventional oxygen sensor systems. Fourth, glucose oxidase is inactivated by hydrogen peroxide, the catalytic

product (24), but we have extended the lifetime of immobilized glucose oxidase by including coimmobilized catalase in excess to prevent peroxide-mediated inactivation (25) and by incorporating a large reserve of the enzymes to maintain a diffusion-limited design (26). These features are not feasible in other glucose sensor designs based on electrochemical detection of hydrogen peroxide (27).

Minimization of Tissue Irritation

The acceptable level of tissue remodeling is also due, in part, to several unique sensor design features. The sensor membrane materials are biocompatible by standard *in vitro* biocompatibility tests (28) and release few, if any, irritants into the tissue. The pore-free PDMS layer prevents passage of current from the electrodes into the tissues and eliminates possible exacerbation of tissue encapsulation due to electrical flux, which may be a problem for some other implanted sensors. In the present design, catalase consumes peroxide, which would otherwise diffuse into adjacent tissues and cause strong irritation. Inclusion of catalase is not possible in other enzyme electrode sensors that are based on hydrogen peroxide detection (27). The implantation method also emphasizes blunt dissection, which is intended to avoid bleeding and minimize damage to the vasculature and lymphatic drains.

Oxygen Access

The stoichiometric shortage of oxygen in tissues with respect to glucose, known as the oxygen deficit (29), can be two or more orders of magnitude. If not resolved, this discrepancy would cause the enzyme reaction in the sensor to be limited by oxygen rather than glucose, and the range of sensitivity to glucose to be substantially reduced. Our sensor design avoids this problem both by salvaging one-half equivalent of oxygen from hydrogen peroxide via the catalase reaction, and by controlling the relative access of substrates to the enzyme region by a novel “two-dimensional” membrane design (8, 9), which permits both radial and axial diffusion of oxygen but only axial diffusion of glucose into the immobilized enzyme gel. These features allow the sensor to respond to glucose over a clinically useful concentration range, even at very low tissue oxygen concentrations.

Variable Microvascular Perfusion

The signals of individual electrodes are affected by convection and diffusion of the substrates, in addition to their concentrations in blood. In tissues, glucose and oxygen are conveyed to the implant site by blood that perfuses the regional microvasculature, then diffuse from capillaries to the sensor. Physiologic variations in blood flow associated with exercise, sleep, movement, hydrostatic changes, and local temperature changes affect the oxygen flux to both the glucose and oxygen reference electrodes simultaneously, as does tissue remodeling, but the signal artifacts associated with these common physiological events are largely subtracted by our differential oxygen detector design. There was limited opportunity to test a range of physiologic variables in the present study, but the capability for artifact subtraction by the sensor can be further assessed in outpatient clinical applications.

Regardless of their respective concentrations in blood, glucose and oxygen are distributed heterogeneously in tissues at the microscopic level (11, 30). As shown in Fig. 5, there is

broad range of oxygen sensor signals between the 10th and 90th percentile limits. Although oxygen sensors are quite uniform in fabrication and produce near-identical signals *in vitro*, when implanted the sensors produce a range of signal values due to the specific microvascular pattern in the immediate neighborhood of each sensor (21). The array of paired glucose and oxygen sensors in the implant potentially provides a means for averaging these local spatial distributions of the substrates, although this feature was not employed in the present study.

Sensor Dynamic Response

A key question is whether an implanted sensor can respond fast enough to follow physiologic blood glucose changes. For this sensor, in which the response of the sensor *per se* is rapid compared to glucose mass transfer within the tissues, the overall rate of response depends on achieving minimal tissue encapsulation and maintaining adequate tissue permeability.

To establish dynamic performance requirements of the sensor, we analyzed archival blood glucose data from stable and unstable diabetic subjects, as well as several non-diabetic controls (31, 32). These data consisted of blood glucose values obtained by regular venous blood collection every 3 to 5 minutes for 24 to 48 hour periods (33). The goal was to identify the most rapid excursions expected in diabetic subjects and identify the characteristics that would be required of a continuously operated sensor to accurately reproduce these excursions. For glucose monitoring based on discrete blood sampling, it was determined that regular sampling at most every 12 to 15 minutes is necessary and sufficient to accurately reconstruct the most rapid physiologic blood glucose excursions, according to the classic Shannon-Nyquist sampling criterion (2 regularly spaced samples/cycle of the most rapid frequency component, 34). This suggests that a continuously operated sensor having a maximal 12 to 15-minute delay should be equally effective in capturing blood glucose excursions. The average 11.8-minute rising and 6.5-minute falling delays seen with this sensor are well within this criterion, indicating that, on average, this system is capable of following all rapid blood glucose excursions expected in the minority of rapid responding diabetic subjects, and by extension, more typical slower excursions in the majority of diabetic subjects.

Results from certain short-term subcutaneous sensor studies in humans have shown comparable delay values. Measurements in some studies have reported delay values from 4 to 10 minutes in humans (19), and an approach based on retrospective correlation between sensor signals and fingerstick assay values estimated a statistical delay of 12.5 minutes (20).

We have also shown that autoregressive moving average (ARMA) methods based on previous blood glucose measurements can predict blood glucose values ahead of real time by as much as 20 minutes with quantifiable accuracy (35). This strategy could be used to further mitigate the effects of delay, if necessary in later applications.

For potential use with an artificial pancreas, the sensor described here is relatively rapid compared to the other components of a closed-loop system, namely, the serial processes of insulin delivery from a pump to a tissue site, insulin adsorption into blood (which, by itself

may be slow compared to the sensor), circulation of insulin and glucose to the peripheral tissues, and activation of the blood glucose change. Therefore, the sensor can have a key role in use of the artificial pancreas to counter hyperglycemic excursions. The convenience of a long-term, fully implanted sensor may also make an artificial pancreas more acceptable to a larger group of people with diabetes. Further, the ability of the sensor to detect and warn of hypoglycemia in a timely fashion will provide an important safety factor in use of automatic blood glucose control systems.

Conclusions

We have shown that, with appropriate design, an implanted glucose sensor can potentially operate effectively for long periods in the body. These experimental results and the understanding of the sensor function derived from animal studies provide a foundation for translation to human clinical investigation.

MATERIALS AND METHODS

Device Implantation

Individual sensor-telemetry units were implanted in subcutaneous tissue sites in 20 kg anesthetized Yucatan minipigs by making an incision 5 cm long and 0.5 – 1 cm deep, retracting the skin, and exposing the dermal layers. A pocket was created between the sub dermal fat and underlying muscle with blunt dissection, while not disturbing the fascia. The implants were placed in this pocket with the sensor surface facing inward towards the muscle layer. Small polyester velour pads were previously fixed to the implant surface to encourage tissue ingrowth and attachment. Once the implant was seated in the pocket, the incision was sutured, and the animal wrapped with a protective bandage. A modified dual-lumen Hickman catheter (Bard Access Systems) was introduced into the central vena cava for blood sampling and fluid infusion, with the catheter ports exteriorized at the midscapular region. The catheter was maintained patent between uses with a dilute solution of heparin. Sterile technique was used in the procedures, and the NIH Guide for the Care and Use of Laboratory Animals was followed for all animal activities.

Glucose Excursion Tests

Glucose excursion tests were performed once or twice weekly. Glucose excursions were achieved by IVGTTs administered by controlled central venous infusion of a 50% glucose solution. In non-diabetic animals, a concomitant infusion of a somatostatin analog (Bachem), was used to partially suppress endogenous insulin production. The results were blood glucose excursions that included a rapid rise from the normoglycemic value (approximately 70 mg/dL) to a plateau of approximately 250 mg/dL, a dwell at the plateau value for approximately 20 minutes, then a rapid unaided fall to the baseline due to the action of endogenous insulin, with occasional mild hypoglycemic undershoot. In diabetic animals, an intravenous insulin bolus was typically used to acutely drop blood levels from starting values of between 200 and 250 mg/dL to nadirs of between 50 and 100 mg/dL, in addition to the IVGTT. Central venous blood was sampled every five to ten minutes during excursions and central venous plasma glucose values were determined using a Yellow Springs Instrument Company (YSI) 2300 STAT Plus glucose analyzer.

Conversion to Diabetic

Pigs were made diabetic by infusion of 85 mg/kg streptozotocin (Axxora). After conversion, animals were maintained on multiple daily subcutaneous and intravenous injections of insulin at typically 0.3 to 0.7 units/kg/day. Blood glucose samples were obtained frequently during the first day following induction of diabetes to assure avoidance of severe hypoglycemia, and multiple times daily thereafter.

Sensor Calibration

As an optimum calibration interval was not known *a priori*, a protocol based on a fixed 10-day interval was employed, utilizing glucose excursions for sensor calibration. The least-squares error between the sensor output and YSI assays of central venous plasma samples was used to determine the values of k1 and k2, and the resulting calibration was then utilized for the following 10 days. Correlation data obtained during a sensor response to a "calibration excursion" were not included in the accuracy determinations. The statistical analyses included only data collected during the sensor responses on days subsequent to calibrations.

Tissue Visualization

Staining of conjugated antibodies employed a labeled streptavidin-biotin immunoenzymatic antigen detection system (36, 37). The stained slides were imaged using an Olympus VANOX-S slide microscope at 40× magnification with an attached Olympus E-30 DSLR with microscope lens mount. The resulting scale factor for the images was 0.34 μm/pixel. Constant exposure and sensitivity settings were maintained during the imaging to maintain identical light levels as indicated by the camera internal light meter. Once a slide was digitally imaged, five regions of 250 μm width and 500 μm depth adjacent to the sensor surface were selected for quantitative histology analysis.

The region visualized was selected at random, but regions with staining artifacts, tissue damage or edge artifacts were avoided. Each image used a combination of color and morphology restrictions to identify stained pixels. These pixels were then divided by the total number of pixels in the image and a quantitative value was obtained.

Acknowledgments

Funding: This work was supported by grants DK64570 and DK77101 (to UCSD) and DK77254 (to GlySens) from the National Institutes of Health. The content is solely the responsibility of the authors and does not necessarily represent the official views of the National Institute of Diabetes and Digestive and Kidney Diseases or the National Institutes of Health.

REFERENCES AND NOTES

1. Zimmet P, Alberti KGM, Shaw J. Global and societal implications of the diabetes epidemic. Nature. 2001; 414:782–787. [PubMed: 11742409]
2. The Diabetes Control and Complications Trial Research Group. The effect of intensive treatment of diabetes on the development and progression of long-term complications in insulin-dependent diabetes mellitus. N. Eng. J. Med. 1993; 329:977–986.
3. Tamborlane WV, Beck RW, Bode BW, Buckingham B, Chase HP, Clemons R, Fiallo-Scharer R, Fox LA, Gilliam LK, Hirsch IB, Huang ES, Kollman C, Kowalski AJ, Laffel L, Lawrence JM, Lee

J, Mauras N, O'Grady M, Ruedy KJ, Tansey M, Tsalikian E, Weinzimer S, Wilson DM, Wolpert H, Wysocki T, Xing D. Juvenile Diabetes Research Foundation Continuous Glucose Monitoring Study Group. N. Eng. J. Med. 2008; 359:1464–1476.

4. Sharkawy AA, Klitzman B, Truskey GA, Reichert WM. Engineering the tissue which encapsulates subcutaneous implants. I. Diffusion properties. J. Biomed. Matls. Res. 1997; 37:401–412.
5. Klonoff DC. Continuous Glucose Monitoring - Roadmap for 21st century diabetes therapy. Diabetes Care. 2005; 28:1231–1239. [PubMed: 15855600]
6. Dassau E, Cameron F, Lee H, Bequette BW, Zisser H, Jovanovič L, Chase HP, Wilson DM, Buckingham BA, Doyle FJ III. Real-time Hypoglycemia Prediction Using Continuous Glucose Monitoring (CGM), A Safety Net to the Artificial Pancreas. Diabetes Care. 2010; 33:1249–1254. [PubMed: 20508231]
7. Armour JC, Lucisano JY, McKean BD, Gough DA. Application of Chronic Intravascular Blood Glucose Sensor in Dogs. Diabetes. 1990; 39:1519–1526. [PubMed: 2245876]
8. Gough, DA.; Lucisano, JY. Membrane and electrode structure for implantable sensor. US Patent. 7,336,984. 2008.
9. Gough DA, Lucisano JY, Tse PHS. A two-dimensional enzyme electrode sensor for glucose. Anal. Chem. 1985; 57:2351–2357. [PubMed: 4061843]
10. Gough, DA.; Jablecki, MC.; Lucisano, JY.; Catlin, MB. Tissue implantable sensors for measurement of blood solutes. US Patent. 7,248,912. 2007.
11. Makale M, Lin JT, Calou R, Tsai A, Chen P, Gough DA. Tissue window chamber system for validation of implanted oxygen sensors. Amer. J. Physiol. 2003; 284:H2288–H2294.
12. FDA-accepted consensus standard "ANSI/AAMI/ISO 14160:1998 – Sterilization of single-use medical devic*es* incorporating materials of animal origin – Validation and routine control of sterilization by liquid chemical sterilants.".
13. McKean BD, Gough DA. A telemetry-instrumentation system for chronically implanted glucose and oxygen Sensors. IEEE Trans. Biomed. Engin. 1988; 35:526–532.
14. Glanz, S. Primer in Biostatistics. 3rd ed.. New York: McGraw-Hill, Inc.; 1992.
15. Parkes JL, Slatin SL, Pardo S, Ginsberg B. A new consensus error grid to evaluate the clinical significance of inaccuracies in the measurement of blood glucose. Diab. Care. 2000; 23:1143–1148.
16. Kovatchev B, Anderson S, Heinemann L, Clarke W. Comparison of the numerical and clinical accuracy of four continuous glucose monitors. Diab. Care. 2008; 31:1160–1164.
17. Garg S, Zisser H, Schwartz S, Bailey T, Kaplan R, Ellis S, Jovanovic L. Improvement in glycemic excursions with a transcutaneous, real-time continuous glucose sensor. Diab. Care. 2006; 29:44–50.
18. Baker DA, Gough DA. Dynamic delay and maximal dynamic error in continuous biosensors. Anal. Chem. 1996; 68:1292–1297. [PubMed: 8651496]
19. Boyne MS, Silver DA, Kaplan J, Saudek CD. Timing of changes in interstitial and venous blood glucose measured with a continuous subcutaneous glucose sensor. Diab. Care. 2003; 52:2790–2794.
20. Kovatchev BP, Shields D, Breton M. Graphical and numerical evaluation of continuous glucose sensing time lag. Diabet. Tech. Thera. 2009; 11:1–5.
21. Makale MT, Jablecki MC, Gough DA. Mass transfer and gas-phase calibration of implanted oxygen sensors. Anal. Chem. 2004; 76:1773–1777. [PubMed: 15018582]
22. Ratner, BD.; Hoffman, AS.; Schoen, FJ.; Lemons, JE., editors. Biomaterials Science: An Introduction to Materials in Medicine. 2nd Edition. San Diego, CA: Elsevier; 2004.
23. Lucisano JY, Armour JC, Gough DA. In vitro stability of an oxygen sensor. Anal. Chem. 1987; 59:736–739. [PubMed: 3565773]
24. Tse PHS, Leypoldt JK, Gough DA. Determination of the intrinsic kinetic constants of immobilized glucose oxidase and catalase. Biotechnol. Bioengin. 1987; 29:696–704.
25. Tse PHS, Gough DA. Time-dependent inactivation of immobilized glucose oxidase and catalase. Biotechnol. Bioengin. 1987; 29:705–713.

26. Gough DA, Bremer T. Immobilized glucose oxidase in implantable glucose sensor technology. Diab. Tech. Thera. 2000; 2:377–380.
27. Jablecki MC, Gough DA. Simulations of the Frequency Response of Implantable Glucose Sensors. Anal. Chem. 2000; 72:1853–1859. [PubMed: 10784153]
28. ISO 10993 - Biological evaluation of medical devices, and FDA Blue Book Memorandum #G95 for Implant Devices with Permanent Contact >30 days with Tissue/Bone.
29. Leypoldt JK, Gough DA. Model of a two-substrate enzyme electrode for glucose. Anal. Chem. 1984; 56:2896–2904. [PubMed: 6524662]
30. Tsai AG, Johnson PC, Intaglietta M. Oxygen gradients in the microcirculation. Physiol. Rev. 2003; 83:933–963. [PubMed: 12843412]
31. Gough DA, Kreutz-Delgado K, Bremer TM. Frequency characterization of blood glucose dynamics. Ann. Biomed. Engin. 2003; 31:91–97.
32. Rahaghi FN, Gough DA. Blood glucose dynamics. Diabet. Tech. Thera. 2008; 10:81–94.
33. Molnar GD, Ackerman E, Rosevear JW, Gatewood lC, Moxness KE. Continuous blood glucose analysis in ambulatory fed subjects. I. General methodology. Mayo Clin. Proc. 1968; 43:833–851. [PubMed: 5710719]
34. Oppenheim, AV.; Schafer, RW. Discrete-time signal processing. Englewood Cliffs, NJ: Prentice-Hall; 1989.
35. Bremer T, Gough DA. Is blood glucose predictable from previous values? A solicitation for data. Diabetes. 1999; 48:445–451. [PubMed: 10078542]
36. Beckstead J. A simple technique for preservation of fixation-sensitive antigens in paraffin embedded tissues. J. Histochem. Cytochem. 1994; 42:1127–1134. [PubMed: 8027531]
37. Vecchi A, Garlanda C, Lampugnani MG, Resnati M, Matteucci C, Stoppacciaro A, Schnurch H, Risau W. Monoclonal antibodies specific for endothelial cells of mouse blood vessels. Their application in the identification of adult and embryonic endothelium. Eur. J. Cell Biol. 1994; 63:247–254. [PubMed: 8082649]

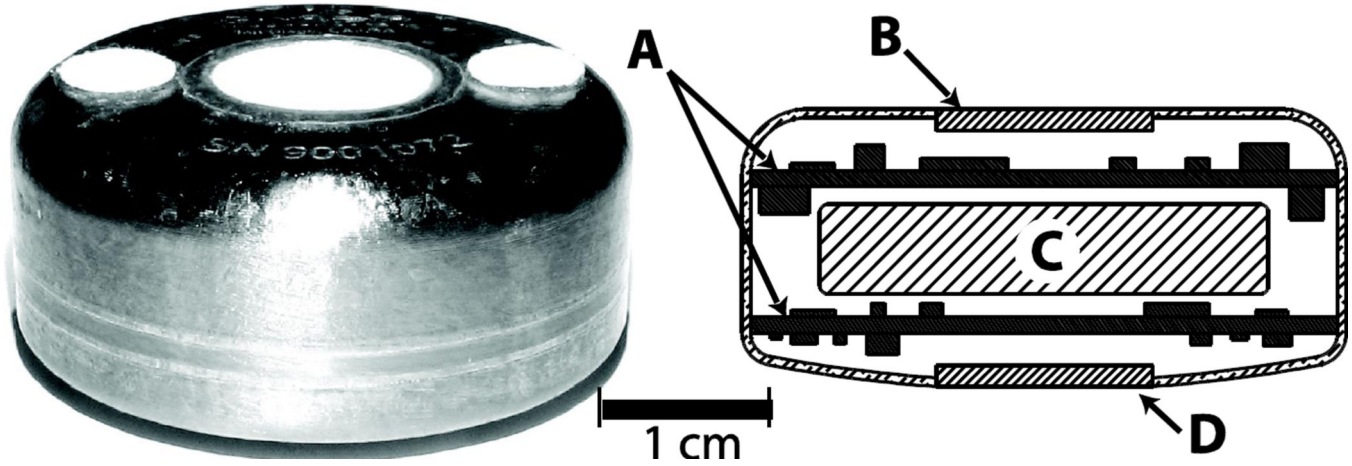

Figure 1. Sensor array with integrated telemetry system prior to implantation

The implant is 3.4 cm in diameter and 1.5 cm thick. The top surface of the implant includes two polyester velour patches for tissue adhesion. Cross-sectional schematic view shows: (A) electronics modules; (B) telemetry transmission portal; (C) battery; and (D) sensor array.

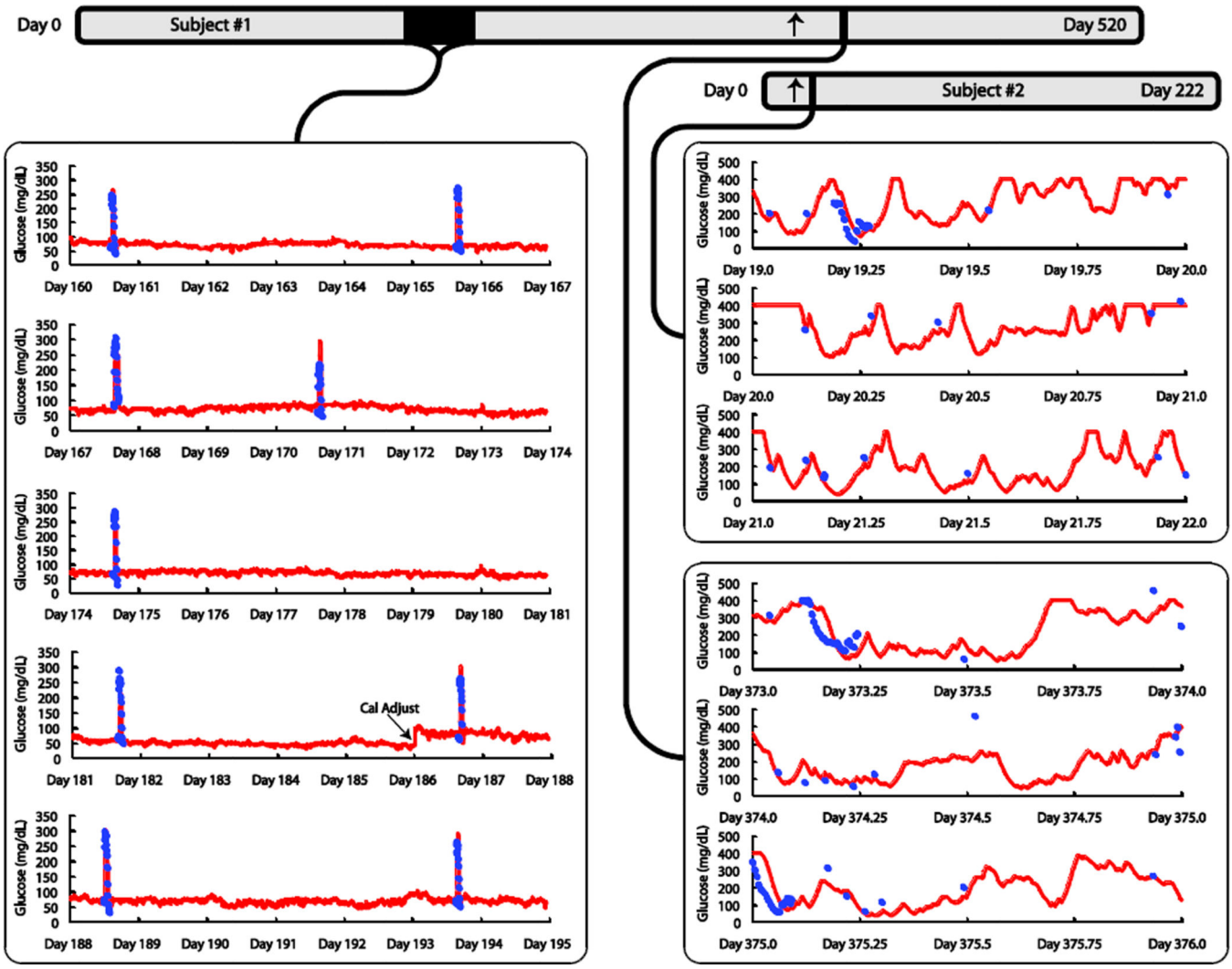

Figure 2. Long-term continuous monitoring in non-diabetic (left panel) and diabetic pigs (right panel)

Timelines for sensor operation in Subjects #1 and #2 are provided at the top; diabetes induction is indicated for each animal by an arrow. Sensor outputs are shown as solid red lines, and plasma glucose values from laboratory analysis (YSI) of central venous samples are shown as solid blue circles. **Left Panel:** The displayed five-week period begins 23 weeks after implantation in Subject #1. Plasma glucose values were sampled during intravascular glucose tolerance tests (IVGTTs) administered once or twice weekly to assess the sensitivity to glucose during the nondiabetic phase. One system calibration adjustment was performed during the entire period (on day 186). Glucose levels are relatively stable between IVGTTs in non-diabetic pigs in spite of eating, and intravenous glucose challenges were required to produce significant glucose excursions. **Right Panel:** The sensor output is shown over two continuous three-day periods in two diabetic pigs. In Subject #1, the sensor had been operated for 352 days with the animal in the non-diabetic state at the time of induction of diabetes, after which monitoring continued for 168 more days. The segment displayed begins on day 373 after sensor implantation (21 days after conversion of the

animal to diabetic). In Subject #2, diabetes was induced 16 days after device implantation, after which monitoring continued for another 206 days. The segment displayed begins on day 19 after sensor implantation (3 days after conversion of the animal to diabetic).

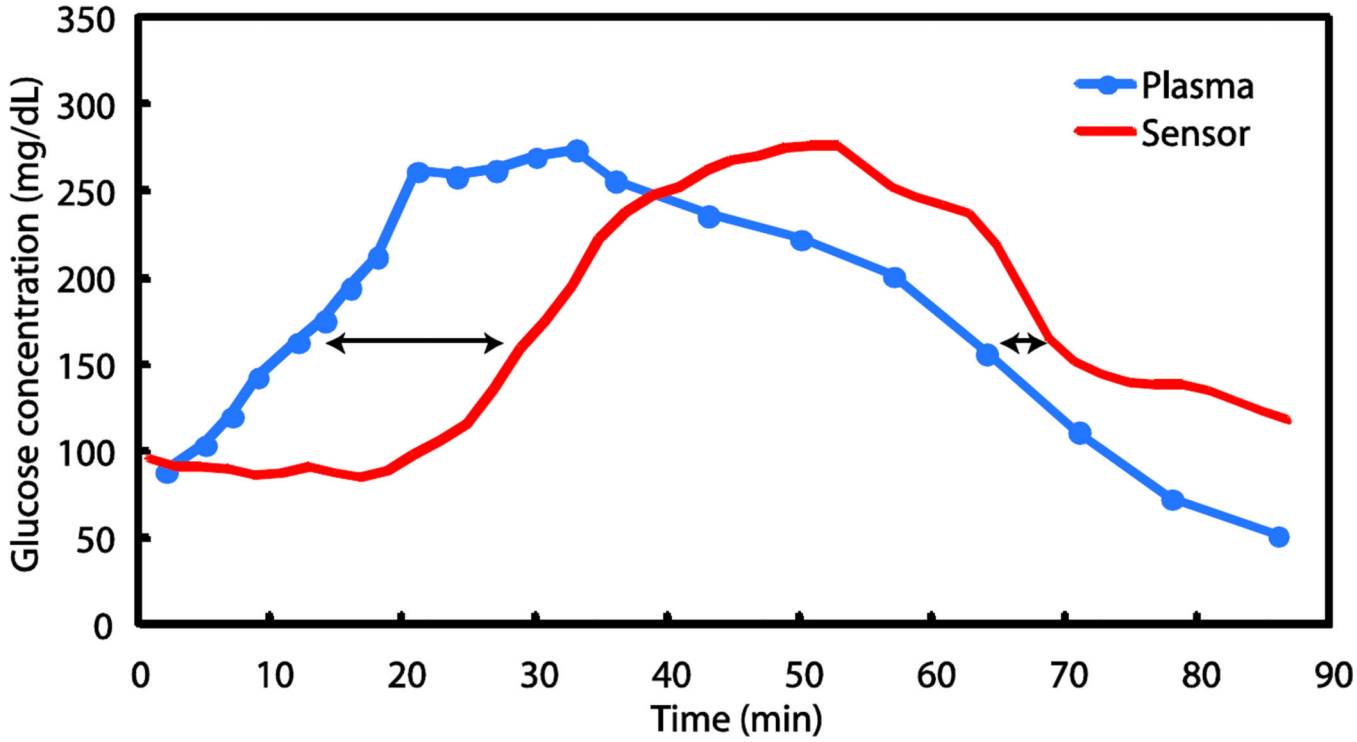

Figure 3. Example of sensor response during an IVGTT excursion

Plasma glucose values in solid blue circles are connected by the blue line and the sensor signal is the red line. The arrows indicate the delay at the 50% points between the minimum and maximum plasma glucose levels for the rising and falling excursions.

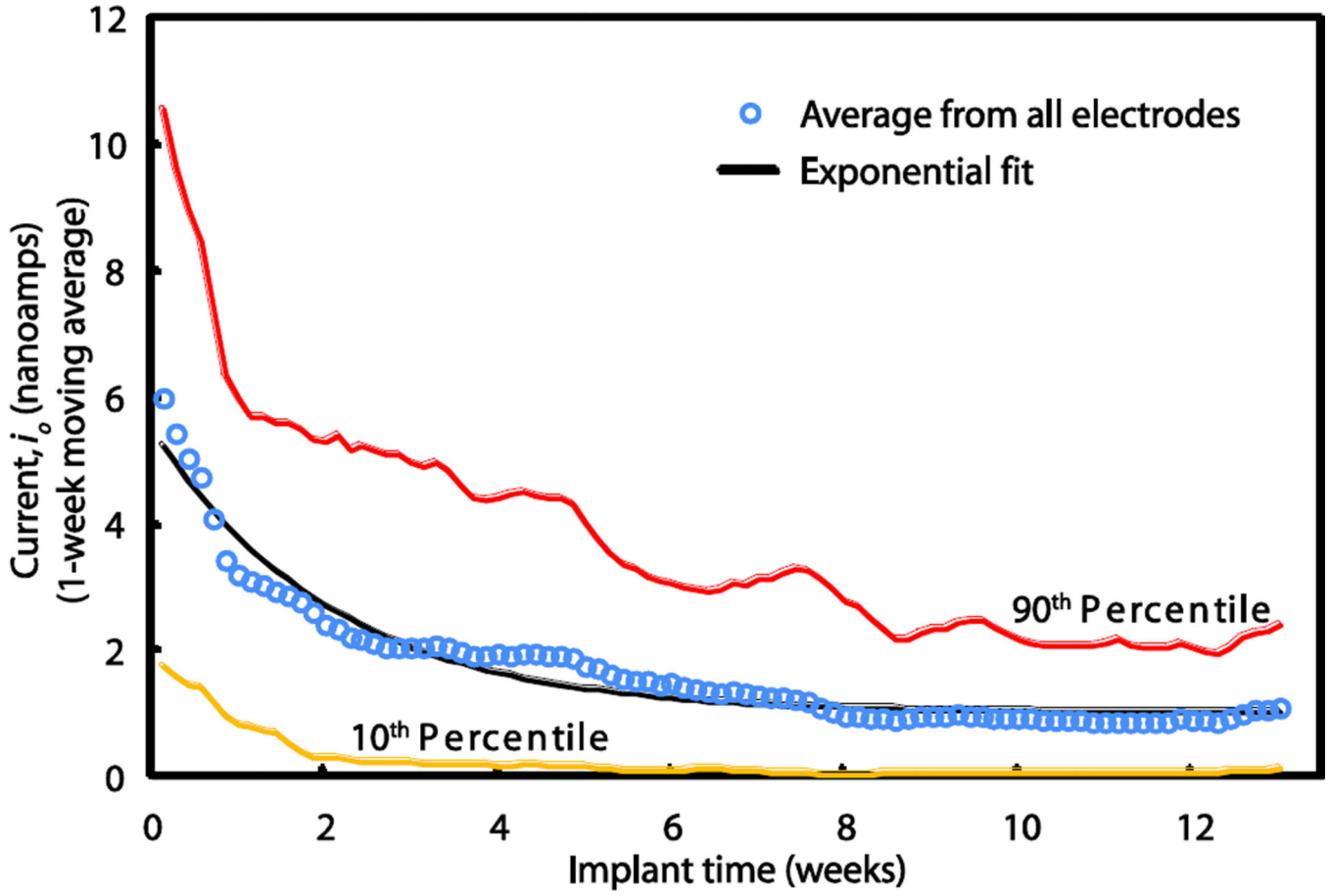

Figure 4. Signals from implanted oxygen sensors over three months

The averaged signal (open circles), expressed as oxygen electrode current in nanoamps, which is proportional to the permeability of the foreign body tissue to oxygen, decays exponentially, approaching an asymptotic constant value at about 6 weeks. The exponential fit (black line) is provided by $i_o = a \cdot e^{-bt} + c$, where a = 4.5 nanoamps, b = 0.49 weeks^{-1}, c = 1.0 nanoamp, and $R^2 = 0.96$. Each data point is an average of the signals from 60 electrodes. Data comprising the 10th and 90th percentiles are represented by the yellow and red lines, respectively.

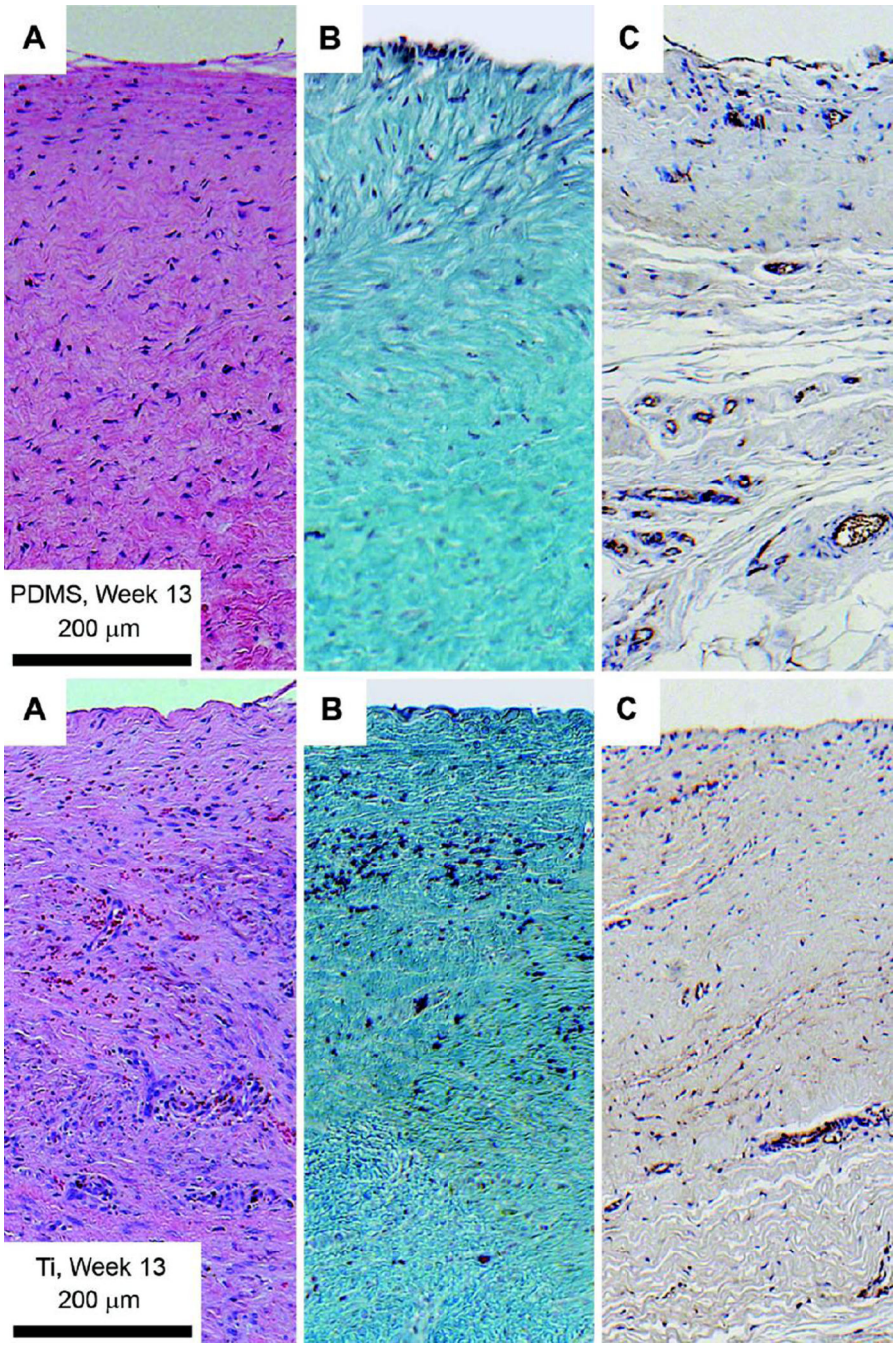

Figure 5. Histology of tissue adjacent to the PDMS surface (upper panels), and Titanium surface (lower panels)

The interface with the implant is above. **(A) H&E stain.** Nuclear features are dark blue/purple, muscle and extracellular spaces are purple/pink, and adipocytes are white. **(B) Gomori Trichrome stain.** Collagen deposits are blue/green, nuclei are dark blue/purple. Red blood cells appear red. **(C) CD31 stain**. CD31 antibodies are dark brown/black, nuclei are blue. Hematoxylin counterstaining of endothelial nuclei appears blue/purple.